Pharm Res (2011) 28:517–530
DOI 10.1007/s11095-010-0298-0

RESEARCH PAPER

A New *In Situ* Brain Perfusion Flow Correction Method for Lipophilic Drugs Based on the pH-Dependent Crone-Renkin Equation

Alex Avdeef • Na Sun

Received: 18 August 2010 / Accepted: 28 September 2010 / Published online: 2 November 2010
© Springer Science+Business Media, LLC 2010

ABSTRACT

Purpose To determine the flow-corrected luminal permeability, P_c, of lipophilic drugs measured by the *in situ* brain perfusion method under circumstances where the traditional Crone-Renkin equation (CRE) method, using diazepam as a flow marker, often fails.

Methods The pH-dependent rate of brain penetration of five lipophilic drugs (amitriptyline, atomoxetine, imipramine, indomethacin, maprotiline, sertraline), as well as of atenolol and antipyrine, were measured in Sprague-Dawley rats. A new pH-dependent CRE was derived and applied to remove the hydrodynamic component of effective permeability, P_e, to produce P_c values.

Results It was shown by the analysis of the *in situ* data in the pH 6.5–8.5 interval for the lipophilic bases that the average vascular flow $F_{pf} = 0.036$ mL·g^{-1}·s^{-1}, centered in a "flow-limit window" (FLW) bounded by $P_e^{min} = 170$ and $P_e^{max} = 776$ (10^{-6} cm·s^{-1} units). It was shown that the traditional CRE is expected not to work for half of the molecules in the FLW and is expected to underestimate (up to 64-fold) the other half of the molecules.

Conclusion The new pH-CRE flow correction method applied to lipophilic ionizable drugs, based on the pH partition hypothesis, can overcome the limitations of the traditional CRE.

KEY WORDS blood-brain barrier · brain permeability-surface area (PS) · crone-Renkin equation · PAMPA-BBB · rodent *in situ* brain perfusion

The current article is contribution number 32 in the Drug Absorption *In Vitro* Model series from pION. Ref. 16 is part 31 in the series.

A. Avdeef (✉) · N. Sun
pION INC
5 Constitution Way
Woburn, Massachusetts 01801, USA
e-mail: aavdeef@pion-inc.com

ABBREVIATIONS

DRW	dynamic range window for flow-limited drugs, $DRW = \log(F_{pf}/S) - \max(\log P_i, \log P_{para})$
FLW	flow limit window: $FLW = \log(F_{pf}/S) \pm 3\ SD = -3.44 \pm 0.33$ (SD = standard deviation)
F_{pf}	cerebrovascular flow velocity of perfusion fluid (mL·g^{-1}·s^{-1} brain tissue)
K_{in}	unidirectional transfer constant (mL·g^{-1}·s^{-1}): $K_{in} = (Q_{br}/C_{pf})/T$, where Q_{br} = test compound parenchymal brain concentration (nmol·g^{-1} brain tissue) (corrected for the vascular volume), C_{pf} = perfusion fluid concentration (nmol·mL^{-1}), T = perfusion time (s).
P_{ABL}	aqueous boundary layer permeability coefficient (cm·s^{-1}), *in vitro* or PAMPA model
P_{app}	apparent *in vitro* transcellular permeability coefficient (cm·s^{-1})
P_c	corrected-for-flow luminal permeability coefficient (cm·s^{-1}) depends on pH for ionizable permeants (hyperbolic function); basis of the pH partition hypothesis
P_c S	permeability-surface area product (mL·g^{-1}·s^{-1}), traditionally determined from K_{in} using Crone-Renkin equation (CRE): $P_cS = -F_{pf}\ln(1 - K_{in}/F_{pf})$
P_e	effective permeability coefficient (cm·s^{-1}), *not* corrected for flow: $P_e = K_{in}/S$ depends on pH for ionizable permeants (sigmoidal function)
pH-CRE	new pH-dependent Crone-Renkin equation (CRE) flow correction method
P_i	luminal permeability coefficient (cm·s^{-1}) of the *ionized* form of permeant
pK_a^{flux}	pH where 50% of the permeation is due to luminal permeability and 50% due to the effective permeability at the hydrodynamic limit

P_m PAMPA transmembrane permeability coefficient ($cm \cdot s^{-1}$), at pH 7.4, corrected for ABL

P_o intrinsic luminal permeability coefficient ($cm \cdot s^{-1}$) of the *neutral* form of permeant for ionizable drugs, $P_o = P_c\left(10^{\pm(pH-pKa)} + 1\right)$, with '+' for acids, '-' for bases

P_{para} paracellular permeability coefficient ($cm \cdot s^{-1}$), indicating aqueous diffusion of permeant through the tight junctions formed by the blood-brain barrier

S endothelial surface area in a gram of brain tissue (assumed to be 100 $cm^2 \cdot g^{-1}$)

INTRODUCTION

The blood-brain barrier (BBB) permeability of a neuropharmaceutical agent can indicate the rate of drug delivery to the brain (1–4). A well-tested method for estimating this permeability is the *in situ* brain perfusion technique (5–7). The initial uptake clearance of a drug perfused into the carotid artery can be represented by K_{in}, the unidirectional transfer constant, which reflects the transport at the luminal BBB membrane. Often, this coefficient is corrected for the effect of hydrodynamic flow from the arterial to the venous side of a microcapillary bed, to yield the permeability-surface area product, $P_c S$ ("corrected-for-flow"). The product of the luminal permeability, P_c ($cm \cdot s^{-1}$), and the endothelial surface area (per gram of brain tissue), S ($cm^2 \cdot g^{-1}$), has commonly been estimated by the Crone-Renkin equation (CRE) (8–10) as $P_c S = -F_{pf} \ln\left(1 - K_{in}/F_{pf}\right)$, where F_{pf} is the cerebral perfusion fluid velocity ($mL \cdot g^{-1} \cdot s^{-1}$), the value of which is determined by a validated flow calibrant, such as diazepam (5–7,11–14).

However, the Crone-Renkin equation can be unreliable when the K_{in} of a test compound is near or higher than the K_{in} (i.e., F_{pf}) of the flow marker diazepam. This has to do with the need for the $1 - K_{in}/F_{pf}$ term in the Crone-Renkin equation to be a positive number and the limits of experimental error. Based on the standard propagation of errors in K_{in} and F_{pf} to the calculated quantity $1 - K_{in}/F_{pf}$, the error in K_{in} would need to be less than the theoretical difference $\left(F_{pf} - K_{in}\right)/\sqrt{2}$ in order for the Crone-Renkin equation to be generally solvable. Given the inter-laboratory variance in permeability measurements (e.g., $\log P_c \pm SD$ values of antipyrine, colchicine, and sucrose are -4.1 ± 0.2, -5.3 ± 0.3, and -6.9 ± 0.5, respectively, with each mean based on 13–21 literature values), the critical condition cannot be generally met by compounds that are near or at the flow limit. Since such molecules would posses $\log K_{in} = \log F_{pf} \pm 0.3$, the Crone-Renkin equation based on accurately-determined diazepam (i.e., positioned near the center of the dispersion) would not work for many of the flow-limited molecules or would produce systematically *underestimated* flow-corrected luminal permeability values.

In the Summerfield *et al.* study (11), where 49 *in situ* rat brain perfusion values were reported, 17 compounds (35%) had K_{in} greater than that of diazepam. In all, possibly as many as 70% of the drugs tested were flow-limited. In the Dagenais *et al.* (12) P-glycoprotein (Pgp)-knockout mouse study, 3 drugs out of 19 also had K_{in} exceed that of diazepam. There are additional examples where diazepam cannot be used for some of the compounds (13,14).

This may be a more common problem than realized in practice in the determination of the luminal BBB permeability of compounds which are close to or are at the flow limit, due to the normal variance of *in situ* brain perfusion measurement. If this hydrodynamic aspect is not correctly factored in, the uptake clearance values determined by the *in situ* perfusion method for flow-dependent drugs would be underestimated (when calculable) and might not reliably correlate with molecular or membrane properties characterizing the rate of penetration into the brain and the subsequent rate of distribution between the brain cellular compartments. Also, *in vitro–in vivo* correlations (IVIVC) could be affected by the likely mismatch of *in vivo* and *in vitro* hydrodynamic characteristics.

Two approaches were explored in this study to overcome the practical limitations mentioned above. First, we sought to identify demonstrably flow-limited molecules, sufficiently soluble in the buffer solutions, whose (flow-corrected) luminal permeability would be greater than that of diazepam, with the aim of providing possible alternatives to diazepam. To verify that the selected molecules were indeed at the flow limit, we selected ionizable drugs which would have shown pH dependence in permeability (15) were they below the flow limit. Second, we explored the pH dependence of the permeation of ionizable compounds possessing high luminal BBB permeability as a way of "self-correcting" for flow, just as had been done successfully in pH-dependent Caco-2 measurements using the so-called 'flux-pK_a' method to correct for the effects of the resistance of the aqueous boundary layer (ABL), a somewhat different hydrodynamic effect associated with planar *in vitro* cell monolayer permeability models (15,16). As far as we are aware, exploitation of the inherent pH dependence in the Crone-Renkin equation had not been done before, although several studies have explored the effects of changes in the pH on the permeability properties of the BBB (17–20).

In this study, the pH-dependent rate of brain penetration of six drugs (amitriptyline, atomoxetine, imipramine, indomethacin, maprotiline, sertraline)—expected to be conditionally flow-limited—were evaluated in male Sprague-Dawley rats using the *in situ* rat brain perfusion technique (5). The Pgp specificity of sertraline and amitriptyline

have been reported to be minimal, with the "Pgp effect" ratios $K_{in}^{knockout}/K_{in}^{wildtype} = 1.2$ and 1.0, respectively (12). The rate of brain penetration for indomethacin was assessed at pH 5.5 and pH 6.5, while those of the lipophilic bases were assessed in the pH interval 6.5 to 8.5. The concentrations of all test and control (atenolol, antipyrine) compounds in the brain were determined by LC-MS/MS. The permeability model analysis indicates a very promising new method to overcome some of the traditional limitations of flow markers such as diazepam.

MATERIALS AND METHODS

Chemicals and Materials

Amitriptyline, antipyrine, atenolol, atomoxetine, imipramine, indomethacin, maprotiline and sertraline were purchased from Sigma-Aldrich (St. Louis, MO, USA) and used as received. Krebs Ringer bicarbonate buffer (KRB), MES (2-(N-morpholino)-ethanesulfonic acid), bicine (N,N-bis(2-hdroxyethyl)glycine), and taurine (2-aminoethanesulfonic acid) were also purchased from Sigma-Aldrich. Standardized solutions used to determine the ionization constants of the drugs were obtained from *p*ION INC.

pK_a Determination at 37°C

The Gemini Profiler (*p*ION) was used to determine the pK_a values of all the ionizable drugs studied here. For each compound, at least three replicate titrations were performed at 37 ± 0.5°C in 1 mL of 0.15 M KCl medium. In order to mimic the physiological condition of the BBB, the new method requires pK_a values at 37°C. The titrated solutions were bathed with argon to minimize the ingress of ambient carbon dioxide. The double-junction pH electrode was calibrated *in situ* using the Avdeef-Bucher (21) four-parameter procedure in the same titration used for the pK_a determination, eliminating the need for traditional "blank" titrations (21,22). Typically, acids are titrated from pH 12.2 to 1.8 with 0.5 M HCl, while bases are titrated from pH 1.8 to 12.2 with 0.5 M KOH. Since most of the drugs studied were only sparingly soluble in water, the 1-propanol (or dimethylsulfoxide) cosolvent procedure (22) was used, where the apparent pK_a values at various ratios of cosolvent (14–43 wt%) were linearly extrapolated to zero-cosolvent to estimate the aqueous value.

In Situ Brain Perfusion Measurement

All of the animal dosing experiments and the LC-MS/MS analyses were performed by Absorption Systems, LP (Exton, PA, USA). The Takasato *et al.* method used here was similar to that published by Summerfield *et al.* (11).

Preparation of Dosing Solutions for in Vivo Study

Perfusate solutions were prepared to contain 3–11 μM of the test compound and two controls: 53–63 μM atenolol (intravascular space marker) (23), 5–7 μM antipyrine (moderate brain permeability marker) (24). Sertraline perfusate solutions at pH 6.5 also contained 5 μM cyclosporine A (CsA). KRB buffer at pH 7.4 was modified to make buffers at pH 5.5, 6.5, 8.0, and 8.5. To prepare pH 5.5 and 6.5 buffers, KRB buffer was supplemented with 10 mM MES and then adjusted to the final pH with 1 M HCl. Buffers at pH 8.0 and 8.5 were prepared by supplementing KRB buffer with 10 mM bicine or taurine and adjusting to final pH with 1 M NaOH. Discrete dosing solutions were prepared for each test compound.

Animal Dosing

Animals used in this study were male Sprague-Dawley rats (300–330 g), obtained from Hilltop Lab Animals, Scottdale, PA. Animals were housed in a temperature-controlled animal facility at West Chester University (West Chester, PA). All of the procedures were approved by the Institutional Animal Care and Use Committee of West Chester University, and they were conducted in accordance with approved standards for laboratory animal care.

Upon arrival, the rats were assigned randomly to treatment groups and acclimated for at least 24 h. Forty-eight rats were used in the study. The animals were supplied with water and a commercial rodent diet *ad libitum* during the study. On the day of the experiment, the rats were anesthetized with a solution containing 50 $mg \cdot kg^{-1}$ ketamine and 3 $mg \cdot kg^{-1}$ xylazine. The left common carotid artery was cannulated with a polyethylene-60 catheter (BD Biosciences, Sparks, MD). Branch arteries were tied, and the cardiac supply was cut off at the start of perfusion.

The perfusion fluid consisted of Krebs-Ringer bicarbonate buffer (KRB), pH adjusted, and was oxygenated with a gas mixture of 95% O_2 and 5% CO_2 prior to the perfusion. The infusion flow rate was 20 $mL \cdot min^{-1}$. Each compound was perfused in four animals. Following the 30-s perfusion, the pump was stopped, and brains were quickly removed from the skull, and the left cerebral hemisphere was excised. Each left hemisphere was placed into a chilled tube, frozen on dry ice, and stored frozen at −60 to −80°C until analysis.

Sample Analysis

Analysis of Brain Samples

The left brain hemisphere from each rat was thawed and weighed. Methanol (20% in water) was added to each left brain hemisphere at about 4 $mL{\cdot}g^{-1}$ of brain tissue, and the mixture was homogenized using sonication with a VirSonic Ultrasonic Cell Disruptor 100 (VirTis).

LC-MS/MS analytical methods for the determination of the test compounds in rat brain homogenate were subjected to a single day, pre-study validation in order to evaluate their accuracy and precision. Samples were introduced into the mass spectrometer by injecting 10 μL of sample through either a PerkinElmer Life and Analytical Sciences (Wellesley, MA) Series 200 HPLC system made up of an autosampler and two micropumps, or on a Leap Technologies (Carrboro, NC) HPLC system made up of a FLUX Instruments quaternary pump and a CTC Analytics HTC PAL autosampler (Presearch, Hitchin, UK). Chromatography was conducted in the reverse-phase mode on either a BDS Hypersil C18, 30×2.1-mm column (3 μm, Thermo-Hypersil Keystone, Bellefonte, PA), an AQUASIL C18, 30×2.1-mm column (3 μm, Thermo-Hypersil Keystone), or a Capcell Pak MF C8, 50×2.0-mm column (5 mm, Phenomenex, Torrance, CA). The aqueous mobile phase consisted of 10% 25 mM ammonium formate buffer at pH 3.5 and 90% water. The organic mobile phase consisted of 10% 25 mM ammonium formate buffer at pH 3.5 and 90% acetonitrile. Analytes were eluted using a gradient of aqueous and organic mobile phase at a flow rate of 300 $\mu L{\cdot}min^{-1}$. Analysis was performed on Applied Biosystems (Foster City, CA) API3000 or API4000 triple quadrupole mass spectrometers equipped with an electrospray source at 450°C and operated in the multiple reaction monitoring (MS/MS) mode. Mass spectrometer parameters were individually optimized for each analyte. Typical run times ranged from 3.5 to 4.5 min.

Acceptance Criteria and Method Validation

One eight-point standard curve and three levels of quality control (QC) samples with six replicates each were analyzed. Standards and QC samples were prepared from independently prepared stock solutions of the test compounds. At least 60% of the standards were required to have accuracy within ±15%, except at the lowest limit of quantification (LLOQ), where ±20% was acceptable. Two-thirds of the batch QCs were required to have accuracy within ±15% of nominal, and at least three QCs were required to pass at each level in order for the run to be accepted. The intra-assay coefficient of variation of the replicate QC determinations were required to be ≤15%, and the accuracy of the mean value for each QC level was required to be within ±15% of the theoretical value. At least four of six QC determinations at each level were required to be available to calculate the statistics.

Calculation of *In Situ* Brain Permeability

The unidirectional transfer constant for the initial brain uptake of the drug, K_{in} ($mL{\cdot}s^{-1}{\cdot}g^{-1}$), was calculated as previously described (5,6):

$$K_{in} = \left[\frac{\left(Q_{tot} - V_{vasc} \cdot C_{pf}\right)/C_{pf}}{T}\right] \quad (1)$$

where Q_{tot} is the total measured quantity of the drug in the brain ($nmol{\cdot}g^{-1}$ brain tissue, both vascular and extravascular) at the end of the perfusion, V_{vasc} is the cerebral vascular volume ($mL{\cdot}g^{-1}$) estimated using atenolol, C_{pf} is the total perfusate concentration of the drug ($nmol{\cdot}mL^{-1}$), and T is the net perfusion time (s). The amount of the drug in the brain parenchyma was determined by subtracting from Q_{tot} the amount of the drug contained in the capillary vascular space (1–2% for the flow-marker compounds). Since a single time point was used, Eq. 1 assumes that uptake is linear with time in the first 30 s of perfusion and that metabolic loss is negligible. Linearity was suggested for most of the compounds from earlier studies done at pH 7.4 (7,11,12).

The value of K_{in} depends on the perfusion flow velocity used in the assay. Highly permeable drugs cannot penetrate the brain any faster than flow velocity permits and are designated as "flow-limited." The Crone-Renkin equation is used to convert the K_{in} values of test compounds to the flow-independent permeability-surface area product value, $P_c\,S$, with F_{pf} defined by the K_{in} of diazepam. In the dependent-variable form, the Crone-Renkin equation is

$$K_{in} = F_{pf}\left(1 - e^{-\frac{P_c S}{F_{pf}}}\right) \quad (2)$$

The pH-CRE (Crone-Renkin Equation) Flow Correction Method

For ionizable molecules, the rate of passive diffusion across the BBB can be interpreted in terms of the pH partition hypothesis: the uncharged form of a drug is expected to have permeability proportional to lipophilicity, and the charged form is expected to be practically impermeable. The fraction of a weak acid/base in the uncharged form depends on the pH of the perfusate and the pK_a of the molecule.

If K_{in} of an ionizable compound (with acid $pK_a<9$ or base $pK_a>5$) were measured at more than one pH, there is an opportunity to determine F_{pf} without the use of standard flow markers, such as diazepam. For such ionizable drugs, the permeability term, P_c, refers to the luminal permeability (commonly at pH 7.4), where the molecule may be partially charged. Usually, the uncharged form of the molecule has a higher 'intrinsic' permeability, P_o, compared to the permeability of the fully ionized form of the molecule, P_i. Carrier-mediated effect, which preferentially favors the charged form of the drug, can increase P_i substantially. For a monoprotic acid or base, the relationship between P_c and pH can be stated as a sum of permeation by three means—as a neutral species (P_o), as a charged species (P_i), and as a leaked species through paracellular water-filled pores in the tight junctions between endothelial cells (P_{para}):

$$P_c = \frac{P_o}{(10^{\pm(pH-pK_a)}+1)} + \frac{P_i}{(10^{\pm(pK_a-pH)}+1)} + P_{para} \qquad (3)$$

where the '±' symbol represents the '−' sign for bases and the '+' sign for acids. The paracellular junctions at the BBB are normally very tight. Since sucrose (342 Da) and inulin (~5600 Da) have typical *in vivo* P_c (paracellular) values of about 0.15 and 0.04×10^{-6} cm·s^{-1}, respectively (26), P_{para} contributions to Eq. 3 can be neglected in most calculations. Also, P_i can be neglected in most calculations, unless the charged form of the drug is a substrate of an uptake transporter.

The *p*CEL-X v3.0 computer program (*p*ION) was used to determine the F_{pf}, P_o and, where possible, P_i or P_{para} (but not both), by a weighted nonlinear regression analysis based on the logarithmic form of Eq. 2, as expanded in Eq. 4:

$$\log K_{in}^{calc}(F_{pf}, P_o, P_i, P_{para}) = \log F_{pf} + \log\left[1 - e^{-\left(\frac{P_o}{(10^{\pm(pH-pK_a)}+1)}+\frac{P_i}{(10^{\pm(pK_a-pH)}+1)}+P_{para}\right)\cdot\frac{S}{F_{pf}}}\right] \qquad (4)$$

The endothelial surface area was assumed to be 100 cm^2·g^{-1} (27). The partial derivatives of the log K_{in} function with respect to the refinable parameters F_{pf}, P_o, P_i, and P_{para}, calculated explicitly in the *p*CEL-X program, based on standard mathematical techniques. The weighted residual's function minimized was

$$R_w = \sum_i^n \left(\frac{\log K_{in,i}^{obs} - \log K_{in,i}^{calc}}{\sigma_i(\log K_{in})}\right)^2 \qquad (5)$$

where n is the number of K_{in} values used in the model refinement, and $\sigma_i(\log K_{in})$ is the standard deviation of the logarithm of the ith measured K_{in}. The effectiveness of the refinement was characterized by the goodness-of-fit, GOF $= [R_w/(n-n_V)]^{1/2}$, where n_V refers to the number of varied parameters. The expected value of GOF is 1 if the model is suitable for the data and the measured standard deviations accurately reflect the precision of the data.

To summarize, the pH-CRE flow correction method can be applied to a flow- or near-flow-limited ionizable drug (whose pK_a value is known at 37°C) (a) by measuring K_{in} in at least two different pH buffers in the pH 5.5–8.5 range, (b) so that molecule is minimally charged in one of the pH buffers and is at or near the flow limit, (c) so that the molecule is substantially charged at the other pH buffer and is well below the flow limit, (d) by analyzing the K_{in} as a function of pH using Eq. 4 to determine the intrinsic permeability, P_o, and (e) by determining P_c at a particular pH using Eq. 3. The method does not require an external flow calibrant such as diazepam. Moreover, the drug chosen for the pH-CRE analysis can also serve as a suitable substitute for diazepam in the traditional CRE method, since the value of F_{pf} is also determined by the analysis (Eq. 4).

Capillary *vs.* Planar Hydrodynamic Effects in Permeability Assays

The capillary-flow CRE, log K_{in} as a function of pH (Eq. 4), has a sigmoidal shape (solid curve in Fig. 1). Similarly, the logarithmic form of the apparent permeability, log P_{app}, as a function of pH for *in vitro* models based on planar

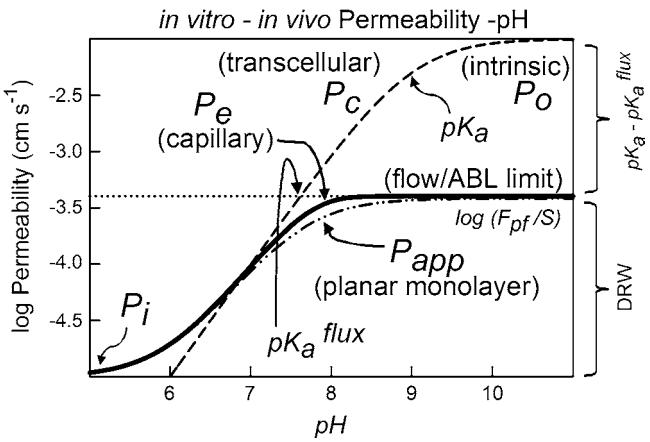

Fig. 1 The characteristics of the capillary- and planar-based equations for a hypothetical moderately lipophilic base molecule with $pK_a=9.0$, log $P_o=-2.0$, log $P_i=-5.0$, $P_{ABL}=-3.4$ (log cm·s^{-1} units), $S=100$ cm^2·g^{-1}, and $F_{pf}=0.04$ mL·g^{-1}·s^{-1} (log(F_{pf}/S) = −3.4). The thick solid curve represents log P_e (=log (K_{in}/S); cf., Eq. 4). The dashed curve represents the transcellular permeability (Eq. 3 with P_i and P_{para} excluded). The horizontal dotted line marks off the permeability limit due to the hydrodynamic effects (flow limit or ABL). The dash-dot-dot curve represents planar cell model log P_{app} (Eq. 6). The pK_a^{flux} value is the pH where 50% of the permeation is due to transcellular permeability and 50% due to the apparent permeability at the hydrodynamic limit.

monolayers of cells (e.g., Caco-2, MDCK) also has a sigmoidal shape (dash-dot-dot curve in Fig. 1). However, the two are not identical. The planar *in vitro* cell permeability model can be expressed by its underlying components: P_{ABL} (aqueous boundary layer permeability) and P_c as

$$\log P_{app} = -\log\left(\frac{1}{P_{ABL}} + \frac{1}{P_c}\right) \quad (6)$$

with P_c defined by Eq. 3 and $P_{ABL}=D_{aq}/h_{ABL}$, where h_{ABL} is the thickness of the aqueous boundary layer (ABL). Values of the aqueous diffusivity, D_{aq}, can be empirically estimated from the molecular weight, MW, as $D_{aq} = 0.991 \times 10^{-6}\mathrm{MW}^{-0.453}\mathrm{cm}^2\cdot\mathrm{s}^{-1}$ at 37°C (28).

Figure 1 illustrates the characteristics of the capillary- and planar-based equations for a hypothetical moderately lipophilic base molecule which has the selected parameters: $pK_a=9.0$, $P_o=0.01$ cm·s^{-1}, $P_i=0.00001$ cm·s^{-1}, $S=100$ cm^2·g^{-1}, and $F_{pf}=0.04$ mL·g^{-1}·s^{-1} ($\log(F_{pf}/S)=-3.40$). For the purpose of comparison of the two hydrodynamic models, the calculation illustrated in Fig. 1 assumes $\log P_{ABL} = -3.40$ (same as $\log (F_{pf}/S)$).

The thick solid curve in Fig. 1 represents $\log P_e$ (=$\log (K_{in}/S)$; cf., Eq. 4). The dashed curve represents the transcellular permeability due to the uncharged species (Eq. 3 with P_i and P_{para} excluded), which is predicted by the pH partition hypothesis. The horizontal dotted line marks off the permeability limit due to the hydrodynamic effects (flow limit or ABL). The dash-dot-dot curve represents planar cell model $\log P_{app}$ (Eq. 6). As can be seen, the main differences between the capillary and planar models occur in the region of the bend in the curve. Both curves have a slope of 1 before the bend and a slope of zero after the bend. The pH in the middle of the bend is called the pK_a^{flux} value (15). This is the pH where 50% of the permeation is due to transcellular permeability and 50% due to the apparent/effective permeability as a consequence of the hydrodynamic effect. This pH is indicated by the point of intersection of the horizontal hydrodynamic-based permeability line (dotted line, Fig. 1) and the diagonal portion of the transcellular permeability curve (dashed curve, Fig. 1). As discussed at greater length elsewhere (15,22,29–31), the value of the intrinsic permeability can be estimated for ionizable flow-limited molecules (i.e., $P_o >> F_{pf}/S$) from $\log P_o = \log\left(F_{pf}/S\right) + \left|pK_a - pK_a^{flux}\right|$.

The solid curve in Fig. 1 indicates the range of possible values which can be directly measured. The dynamic range window (DRW) of direct measurements of permeability is defined by the difference between the maximum possible value at the top of the solid curve ($P_e^{max} = F_{pf}/S$) and the minimum possible value at the bottom of the fully shown sigmoidal curve (P_e^{min}=maximum of P_i and P_{para}).

PAMPA-BBB Values

In this study, the literature values of K_{in} for 132 molecules were compared to the corresponding passive permeability values based on an artificial membrane model, with the latter values calculated using the computer program *p*CEL-X (*p*ION). The parallel artificial membrane permeability assay (PAMPA) based on membranes formed from 10% w/v porcine brain extract dissolved in an alkane, PAMPA-BBB, described by Tsinman *et al.* (34), has its prediction encoded into *p*CEL-X so that values of membrane permeability at pH 7.4, $P_m^{\text{PAMPA-BBB}}$, can be estimated from 2D structures ('mol' file format) alone. For the drugs whose *in situ* data were measured in this study, experimental intrinsic PAMPA-BBB values, $P_o^{\text{PAMPA-BBB}}$, were taken from Tsinman *et al.* (34).

RESULTS AND DISCUSSION

pK_a Determinations

Table I lists the physical properties of the molecules considered, including the 37°C pK_a values determined in this study. The experimental octanol-water partition coefficients are taken from common sources (22). Since many of the molecules considered are only sparingly soluble, the pK_a values were determined in the mixed solvent approach (22). The choice of water-miscible organic solvents was dictated by the concern for elevated volatility at 37°C. The use of methanol (or similarly volatile solvents) is not recommended, since the steady rate of its evaporation leads to difficult-to-recognize systematic inaccuracies in the extrapolated values of the ionization constants. Typically, the pK_a values of bases are about 0.3 log units lower at 37°C, compared to values at 25°C; usually, the pK_a values of acids are less affected by temperatures (32).

In Situ Rat Brain Perfusion Measurement Results

Two groups of *in situ* rat brain perfusion measurements were performed at different times, designated as the "A" and "B" dosing groups in Tables II and III. In the A dosing group, indomethacin at pH 5.5 and 6.5 and sertraline at pH 6.5 and 8.5 were measured in quadruplicate (16 rats). Sertraline was perfused in the presence of 5 μM CsA, a potent inhibitor of Pgp. The rest of the molecules (B dosing group) were measured several months later, at pH 7.4, 8.0, and 8.5 (32 rats). Sertraline at pH 8.5 was repeated in group B at 2.9 μM concentration and in the absence of CsA, on the hunch that the group-A pH 8.5 measurement

Table I Physical Properties

Compound	MW	log P_{OCT}	log $P_o^{PAMPA-BBB}$	pK_a (37°C)	GOF	n	Ref	Mixed-Solvent (0.15 M KCl) for pK_a determination
Amitriptyline	277	4.6	−1.2	8.92±0.10	6.4	3	[a]	15–31 wt% 1-propanol
Antipyrine	188	0.6	−5.3	–	–	–	–	–
Atenolol	266	0.2	−5.3	9.19±0.01	1.9	6	32	aqueous
Atomoxetine	255	3.3	−1.8	9.50±0.05	1.4	3	[a]	25–43 wt% 1-propanol
Diazepam	285	2.8	−3.8	–	–	–	–	–
Imipramine	280	4.4	−1.5	9.23±0.06	7.0	3	[a]	19–33 wt% dimethylsulfoxide
Indomethacin	358	3.5	−2.7	4.27±0.08	3.9	5	33	aqueous and 12–35 wt% 1-propanol
Maprotiline	277	5.1	−0.6	10.01±0.01	0.7	3	[a]	19–33 wt% dimethylsulfoxide
Sertraline	306	4.9	−1.7	8.85±0.09	2.8	3	[a]	15–31 wt% 1-propanol

$logP_{OCT}$ are measured octanol-water partition coefficients taken from multiple sources (22). Values of $logP_o^{PAMPA-BBB}$ are measured PAMPA values (34) based on 10% porcine brain extract lipids dissolved in an alkane artificial membrane barrier. GOF is the goodness-of-fit for the pKa refinement based on n mixed-solvent titrations. [a] This work—potentiometric analysis using the Gemini Profiler (*p*ION)

of 10 μM sertraline and in the presence of CsA may have been mitigated by some precipitation of the drug. Since the repeated value was appreciably higher, the first value was discarded.

Vascular Space Determination

Table II summarizes the atenolol perfusion data. Following perfusion, the vascular space marked by atenolol, a compound that does not penetrate the brain except by very small paracellular leakage (log P_{para} −7.25, Fig. 2c), ranged from 6.9 to 19.1 $\mu L \cdot g^{-1}$ (excluding two outliers). In the interval pH 5.5–7.4, two atenolol replicates (V_{vasc} 28.5 and 77.6 $\mu L \cdot g^{-1}$) were excluded from the final average data, based on their high vascular volumes (Dixon's Q-test, 95% confidence limit). Of the 14 accepted measurements, the average V_{vasc} values at pH 5.5, 6.5, and 7.4 were 12.9± 3.0, 13.0±4.1, and 13.9±0.1 $\mu L \cdot g^{-1}$, respectively. The pH 5.5 and 6.5 vascular volumes were used to make corrections to all the other measurements, according to Eq. 1. Averaged over the pH 5.5–6.5 interval (A-1 to A-3, Table II), the apparent vascular space volume in this study was 13.0±3.7 $\mu L \cdot g^{-1}$ brain tissue (average±SD; n=11), which is in agreement with the sucrose intravascular volume reported by Smith *et al.* (25) and many other investigators. It appears that the non-physiological pH values used in the perfusate solutions did not exhibit abnormal vascular volume, as directly indicated by atenolol for pH 5.5–7.4 and indirectly suggested by the antipyrine permeability for pH>7.4.

The atenolol data at pH 8.0 and 8.5 were not used for vascular space determination, but rather were treated as were the data for the test drugs. Table II shows K_{in} values of atenolol in the slightly alkaline pH 8.0 and 8.5 solutions, corrected for vascular volume using the pH 5.5–6.5 atenolol data. Although the values are small, they appear to be consistent with the predictions of the pH partition hypothesis (Fig. 2c). The *in situ* brain perfusion permeability of atenolol had not been reported in the literature before this study.

Table II *In Situ* Brain Perfusion Controls

Compound	Dosing group	pH	Concn (μM)	K_{in}(10^{-4} mL.g^{-1}.s^{-1})
atenolol	A-1	5.5[a]	53.3	–[d]
	A-2	6.5[a]	52.6	–[d]
	A-3	6.5[a]	63.4	–[d]
	B-5	7.4	61.7	0.3±0.1
	B-1	8.0[b]	63.3	–[e]
	B-3	8.0[b]	63.2	0.2±0.9
	B-7	8.0[b]	58.1	0.2±1.5
	B-2	8.5[b]	57.0	–[e]
	A-4	8.5[c]	54.6	3.5±5.2
	B-4	8.5[b]	62.1	0.5±1.4
	B-6	8.5[b]	56.4	0.1±0.3
	B-8	8.5[b]	57.0	0.5±7.7
antipyrine	A-1	5.5[a]	6.7	58±5
	A-2	6.5[a]	6.1	50±7
	A-3	6.5[a]	6.8	50±22
	A-4	8.5[c]	6.8	42±12
	B-1	8.0[b]	5.5	67±13
	B-2	8.5[b]	6.4	48±12
	B-3	8.0[b]	5.7	75±7
	B-4	8.5[b]	5.0	77±10
	B-5	7.4	5.6	82±23
	B-6	8.5[b]	5.7	80±15
	B-7	8.0[b]	5.8	72±12
	B-8	8.5[b]	6.1	70±5

"±" precedes the standard deviation, based on n=4 rats, except n=3 in Dosing Group A-1 and B-5. [a] 10 mM MES added to the KRB buffer. [b] 10 mM bicine added to the KRB buffer. [c] 10 mM taurine added to the KRB buffer. [d] Used to define average vascular space volume. [e] Excluded since vascular space correction produces a negative number

Table III *In Situ* Transfer Constants for the Flow-Limited Drugs

Compound	Dosing group	pH	Concn (μM)	K_{in} (mL.g^{-1}.s^{-1})
Indomethacin	A-1	5.5[a]	7.3	0.032 ± 0.008
	A-2	6.5[a]	7.8	0.004 ± 0.001
Sertraline	A-3	6.5[a,c]	9.7	0.035 ± 0.023
	B-4	8.5[b]	2.9	0.037 ± 0.015
Amitriptyline	B-1	8.0[b]	11.0	0.044 ± 0.013
	B-2	8.5[b]	10.1	0.045 ± 0.014
Atomoxetine	B-3	8.0[b]	9.9	0.026 ± 0.010
	B-4	8.5[b]	9.6	0.032 ± 0.015
Imipramine	B-5	7.4	11.5	0.031 ± 0.021
	B-6	8.5[b]	11.0	0.032 ± 0.002
Maprotiline	B-7	8.0[b]	10.8	0.052 ± 0.011
	B-8	8.5[b]	10.9	0.036 ± 0.013

Each dosing group consisted of n = 4 rats. In two of the groups, n = 3 (a measurement was rejected due to high atenolol volumes of distribution). By comparison, the diazepam K_{in} values reported in the literature include 0.033 and 0.043 mL.g^{-1}.s^{-1} (11,12). "±" precedes the standard deviation. [a] 10 mM MES added to the KRB buffer. [b] 10 mM bicine added to the KRB buffer. [c] 5 μM CsA added to the KBR buffer

Antipyrine as a Control

Table II summarizes the antipyrine perfusion data. The K_{in} values of antipyrine, a moderate brain penetration marker, ranged from 0.0042 to 0.0082 mL·g^{-1}·s^{-1}, and were in reasonable agreement with published values (11). The A dosing group had a slightly lower average value than the B dosing group (0.0050 ± 0.0007 and 0.0072 ± 0.0010 mL·g^{-1}·s^{-1}, respectively). There was no systematic pH dependence to the antipyrine K_{in} values (Fig. 2b). This observation, taken with the atenolol vascular volume estimates, suggests that the integrity of the BBB was maintained over the 30-s perfusion period even though the pH of the perfusate was non-physiological.

The pH Dependence of the Ionizable Drugs

Table III summarizes the *in situ* brain perfusion results for the drugs studied in the interval pH 5.5–8.5. Figure 2 shows plots of the log permeability *vs.* pH for the measured drugs. Literature K_{in} data (11) at pH 7.4 for amitriptyline, atomoxetine, maprotiline, and sertraline were included with the measurements reported here in the regression analysis (Table IV).

The K_{in} of indomethacin decreased with increasing pH. At pH 5.5, indomethacin had an average K_{in} of 0.032 ± 0.008 mL·g^{-1}·s^{-1}, while at pH 6.5, the average K_{in} decreased to 0.0042 ± 0.0008 mL·g^{-1}·s^{-1} (Fig. 2f). The K_{in} of sertraline very slightly increased with increasing pH. At pH 6.5, the K_{in} for sertraline was 0.035 ± 0.022 mL·g^{-1}·s^{-1}, while at pH 8.5, it was 0.037 ± 0.015 mL·g^{-1}·s^{-1} (Fig. 2h). The other weak bases followed a similar trend, with very little pH dependence in the alkaline interval studied. Given the pK_a values of the weak bases, the absence of the steep pH dependence (as that seen with indomethacin and atenolol in Fig. 2) was strong evidence that the weak bases were at the flow limit.

Refinement of the K_{in} – pH Data

Table IV summarizes the results of the weighted nonlinear regression analysis based on Eq. 4. The solid curves in Fig. 2 depict the best-fit of log (K_{in} / S) values as a function of pH. The dashed hyperbolic curves represent the luminal permeability, log P_c, as a function of pH. These follow the pH dependence according to the pH partition hypothesis. For flow-limited molecules, the Crone-Renkin equation is theoretically expected to transform the solid (effective) curve to that represented by the dashed (luminal) curve. The unfilled circles in Fig. 2 represent the ideally corrected P_c values, if the Crone-Renkin equation were to use error-free K_{in} values, and F_{pf} values were precisely known.

Table IV lists the refined F_{pf}, P_o, and P_i parameters. There were only enough data for the weak bases (n = 2 − 3, Table IV) to refine just one or two parameters. All of the measured lipophilic bases were flow-limited in the pH 7.4–8.5 interval. Maprotiline showed some luminal pH dependence at pH 7.4, as did sertraline at pH 6.5.

In addition to the compounds studied here, the Okura *et al.* (20) study of the *in situ* rat brain perfusion of oxycodone at pH 7.4 and 8.4 (using the infusion flow rate of 4.9 mL·min^{-1} over a 30-s time interval) was subjected to the regression analysis, primarily to use it as an example of the pH partition hypothesis. Specifically, the 1 mM pyrilamine inhibitor case was examined, where the carrier-mediated process was largely saturated.

Amitriptyline

The two K_{in} values determined in this study and a third value taken from the literature (11) allowed the determination of $F_{pf} = 0.051 \pm 0.003 \text{mL} \cdot \text{g}^{-1} \cdot \text{s}^{-1}$. Since the K_{in} at pH 7.4 (the lowest pH) was still flow-limited

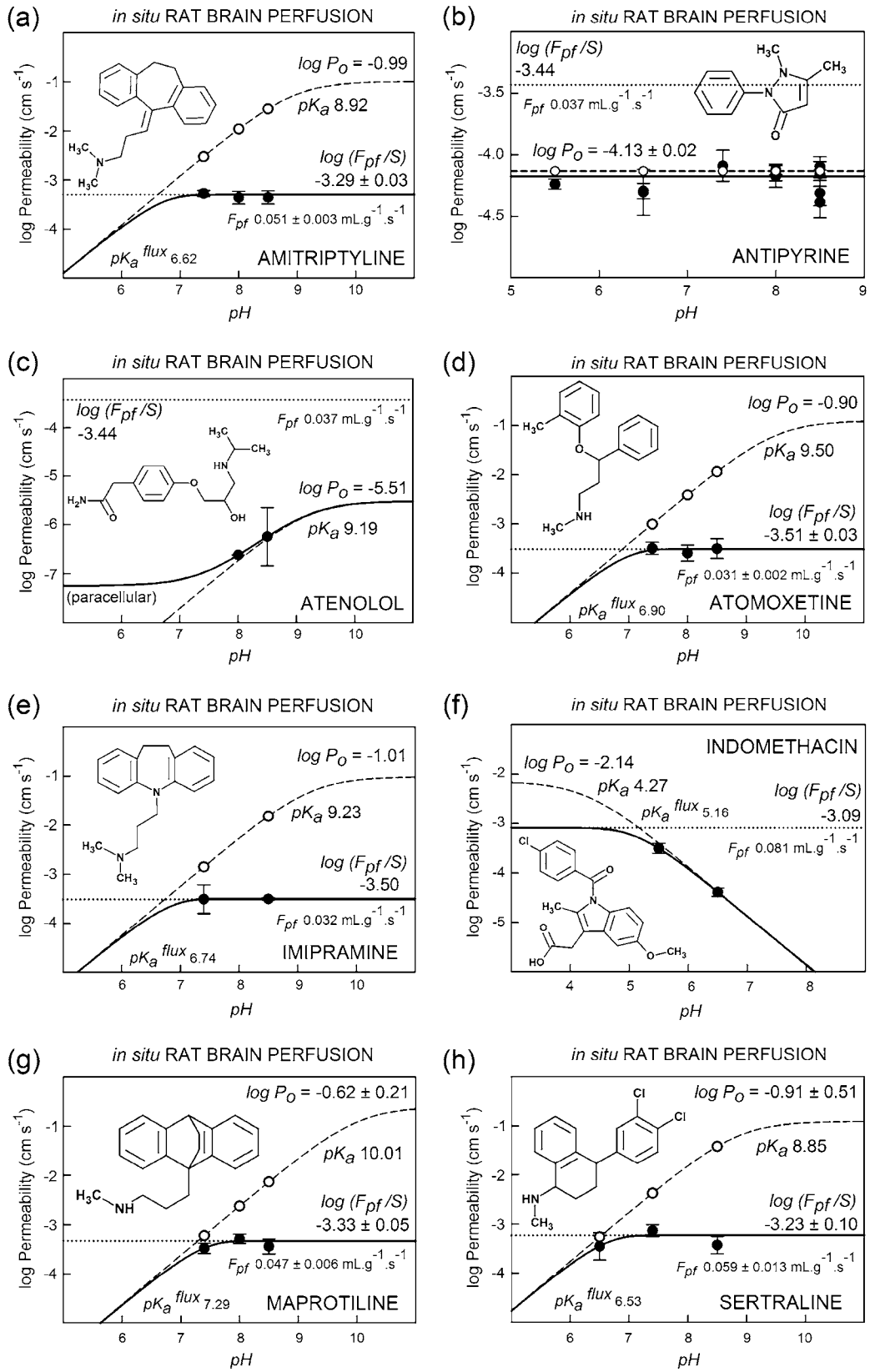

Fig. 2 Plots of the log permeability *vs.* pH for the measured drugs, including literature data at pH 7.4 for amitriptyline, atomoxetine, maprotiline, and sertraline (cf., Table IV). The curve types have been defined in Fig. 1. The solid curves depict the best-fit of log (K_{in} /S) (= log P_e) values as a function of pH. For flow-limited molecules, the Crone-Renkin equation is theoretically expected to transform the solid (effective) curve to that represented by the dashed (luminal) curve. The unfilled circles represent the P_c values determined by the pH-CRE method.

Table IV Refinement Results—Unidirectional Transfer Constants as a Function of pH

Compound	pH	log(K_{in}/S)	Ref	F_{pf} (mL.g^{-1}.s^{-1})	log P_o	log P_i	P_cS (CRE)	P_cS (pH-CRE)	GOF	n
Amitriptyline	7.4	−3.27 ± 0.06	11	0.051 ± 0.003	−0.99[d]		–[c]	2997	0.5	3
	8.0	−3.35 ± 0.13	[a]				549	10,974		
	8.5	−3.35 ± 0.13	[a]				–[c]	28,173		
Antipyrine	5.5	−4.24 ± 0.04	[a]	0.036[e]	−4.13 ± 0.02		63	77	1.2	12
	6.5	−4.30 ± 0.12	[a]				54	77		
	7.4	−4.09 ± 0.13	[a]				92	77		
	8.0	−4.15 ± 0.06	[a]				80	77		
	8.5	−4.21 ± 0.08	[a]				70	77		
Atenolol	8.0	−6.62 ± 0.00	[a]	0.036[e]	−5.51	−7.25	0.24	0.24		2
	8.5	−6.24 ± 0.60	[a]				0.57	0.58		
Atomoxetine	7.4	−3.49 ± 0.12	11	0.031 ± 0.002	−0.90 [e]		–[c]	805	0.4	3
	8.0	−3.59 ± 0.16	[a]				549	3134		
	8.5	−3.50 ± 0.20	[a]				–[c]	9295		
Imipramine	7.4	−3.50 ± 0.29	[a]	0.032	−1.01		1437	1416		2
	8.5	−3.50 ± 0.03	[a]				2150	15,260		
Indomethacin	5.5	−3.50 ± 0.10	[a]	0.081	−2.14		400	399		2
	6.5	−4.39 ± 0.08	[a]				42	42		
Maprotiline	7.4	−3.48 ± 0.11	[a]	0.047 ± 0.006	−0.62 ± 0.21		580	591	0.6	3
	8.0	−3.29 ± 0.09	[a]				–[c]	2335		
	8.5	−3.44 ± 0.15	[a]				691	7234		
Oxycodone [c]	7.4	−4.78 ± 0.03	20	0.126	−3.59	−5.47	17	17		2
	8.4	−4.04 ± 0.05	20				94	95		
Sertraline	6.5	−3.45 ± 0.28	[a]	0.059 ± 0.013	−0.91 ± 0.51		537	545	1.0	3
	7.4	−3.14 ± 0.12	11				–[c]	4202		
	8.5	−3.43 ± 0.18	[a]				590	37,881		

K_{in} is the unidirectional transfer constant (mL.g^{-1}.s^{-1}). The endothelial surface area, S = 100 cm^2·g^{-1} assumed. The intrinsic (neutral molecule) permeability is represented by P_o (cm.s^{-1}). The permeability of the ionized species is represented by P_i (cm.s^{-1}). P_c (cm.s^{-1}) is the transendothelial permeability at a particular value of pH. GOF = goodness-of-fit in the n-point weighted nonlinear regression analysis based on Eq. 4. F_{pf} is the cerebrovascular flow velocity (mL.g^{-1}.s^{-1}). P_cS calculation based on traditional CRE method and the new pH-CRE method. [a] This work. [b] 30 μM sample + 1 mM pyrilamine inhibitor. [c] Traditional CRE failed since $1 - K_{in}/F_{pf} < 0$. [d] Estimate of the minimum value. [e] Weighted mean value

(Fig. 2a), the estimated log P_o is expected to be≥ −0.99. Any entry of lower values would have raised the value of the GOF in the refinement (Table II). (It would have been necessary to have additional K_{in} measurements at pH 6.0 or 5.5 to determine a more precise value of log P_o.) The CRE based on the refined value of F_{pf} does not work at pH 7.4 and 8.5 and underestimates the P_cS value at pH 8.0 by a factor of 20 (Table IV). The P_cS values determined by the pH-CRE method (Eq. 3 incorporating the P_o from Eq. 4 refinement) are listed in Table IV and shown in Fig. 2a as log P_c unfilled circles along the dashed curve.

Antipyrine

Since antipyrine is well below the flow limit (Fig. 2b), the regression analysis used the average value of F_{pf} determined by the lipophilic weak bases as a fixed contribution. The value of P_o was determined by regression as −4.13 ± 0.02 (GOF 1.2, n = 12). This value compares well with those reported in the literature. The CRE flow-corrected values and those based on calculated P_c using Eq. 3 (Table IV) agree well. The lack of any systematic pH dependence in the K_{in} values of the control compound suggests that the BBB integrity is not compromised at non-physiological pH in the 30-s perfusion duration.

Atenolol

The BBB permeability of atenolol had not been reported before. Hence, atenolol was both a control and an object of permeability determination. The pH 5.5 and 6.5 data were used to determine the average vascular volume, which was used as a correction term (Eq. 1) in all the other measurements, including those of atenolol at pH 8.0 and 8.5. The multiple measurements of atenolol at the latter two values of pH were log-averaged and used in the regression analysis based on Eq. 4. Since atenolol is well below the flow limit, the average value of F_{pf} determined by the lipophilic weak bases was included as a fixed contribution in the calcula-

tion. With two knowns, it was possible to determine two unknowns: log P_o= −5.51 and log P_{para}= −7.25. Fig. 2c demonstrates that the pH dependence follows the pH partition hypothesis above pH 8 and in acidic pH shows the expected deviation due to the small leakage through the paracellular aqueous pores in the BBB (asserting that the molecule is not a significant substrate for a cation transporter, since its determined P_{para} value is very close to the permeability of sucrose and inulin).

Atomoxetine

The two K_{in} values determined in this study and a third value taken from the literature (11) allowed the determination of $F_{pf} = 0.031 \pm 0.002 \text{mL} \cdot \text{g}^{-1} \cdot \text{s}^{-1}$. Since the K_{in} at pH 7.4 (the lowest pH) was still flow-limited (Fig. 2d), the estimated log P_o is expected to be ≥ −0.90. Any entry of a lower value during refinement would have raised the value of the GOF (Table II). The traditional CRE based on the refined value of F_{pf} does not work at pH 7.4 and 8.5 and underestimates the P_eS value at pH 8.0 by a factor of 6 (Table IV).

Imipramine

The two K_{in} values reported here allowed the determination of F_{pf}=0.032 mL·g $^{-1}$·s $^{-1}$ and log P_o= −1.01 (errors could not be deduced since the refinement was not "overdetermined," i.e., there were two knowns and two unknowns). The traditional CRE based on the refined value of F_{pf} yielded at pH 7.4 a P_eS values that agreed with the expectations of the pH partition hypothesis, but the value at pH 8.5 was underestimated by a factor of 7 (Table IV).

Indomethacin

The two K_{in} values determined in this study allowed the determination of F_{pf}=0.081 mL·g $^{-1}$·s $^{-1}$ and log P_o= −2.14. The pH 5.5 K_{in} is just slightly flow-limited, but the value at pH 6.5 is not appreciably affected by flow. The two points in Fig. 2 illustrate the expected trend according to the pH partition hypothesis. The traditional CRE produces reasonable (small) corrections for the two points (Table IV). The present results could not be reconciled with the pH 7.4 value reported by Parepally *et al.* (7), whose K_{in} value suggests a log P_o an order of magnitude higher than that determined here. From self-inhibition studies, there was no evidence of saturable transporter effects at pH 7.4 (7).

Maprotiline

The two K_{in} values reported here and the literature value (11) allowed the determination of $F_{pf} = 0.047 \pm 0.006 \text{mL} \cdot \text{g}^{-1} \cdot \text{s}^{-1}$ and $\log P_o = -0.62 \pm 0.21$ for maprotiline. This molecule has the highest intrinsic permeability of the drugs studied and is among the highest reported in the literature. The traditional CRE using the refined F_{pf} yields a reasonable P_eS value at pH 7.4, does not work at pH 8.0, and underestimates the pH 8.5 value by a factor of 11 (Table IV).

Oxycodone

The analysis of the K_{in} data of Okura *et al.* (20) of 30 μM oxycodone in the presence of 1 mM pyrilamine inhibitor produced log P_o= −3.59 and log P_i= −5.47, using F_{pf}= 0.126 mL·g $^{-1}$·s $^{-1}$ reported by Okura. The intrinsic value is not sensitive to the flow limit conditions, based on the reported value of F_{pf}. Like that of atenolol and indomethacin, the pH dependence of the two K_{in} values of oxycodone illustrates the expected trend according to the pH partition hypothesis.

Sertraline

The two K_{in} values reported here and the one taken from the literature (11) allowed the determination of $F_{pf} = 0.059 \pm 0.013$ and $\log P_o = -0.91 \pm 0.51$ for sertraline. The traditional CRE based on the refined value of F_{pf} yields a reasonable P_eS value at pH 6.5, does not work at pH 7.4, and underestimates the value at pH 8.5 by a factor of 64 (Table IV).

The Challenge of Applying the Traditional CRE to Lipophilic Molecules

Figure 2 indicates that the log P_e at the flow limit includes permeability values at pH 7.4, 8.0, and 8.5 for amitriptyline, atomoxetine, imipramine, and sertraline and at pH 8.0 and 8.5 for maprotiline. A plot of these is shown in Fig. 3. The solid line represents the weighted mean $\log\left(F_{pf}/\text{S}\right) -3.44 \pm 0.11 \left(F_{pf} 0.036 \pm 0.009 \text{mL} \cdot \text{g}^{-1} \cdot \text{s}^{-1}\right)$ based on the above 12 points. The dashed lines represent a range based on ±3 standard deviations, marking the proposed flow limit window (FLW) to be expected for data compiled from different laboratories. Values of reported F_{pf} [rodent / mL·min $^{-1}$ flow rate] from various laboratories include 0.043 [mouse/2.5] (12), 0.071 [rat and mouse/1.0] (35), 0.069 [rat/4.5] (36), 0.040 [rat/4.0] (37), 0.070 [rat/10.0] (38), and 0.050 [mouse/2.5] (39) mL·g $^{-1}$·s $^{-1}$. In addition to the flow rate, the surgery method plays a role in the resulting vascular flow rate.

Figure 4 shows such an inter-laboratory plot of 132 published *in situ* brain perfusion effective (*not* corrected for flow) permeability, $\log P_e (= \log(K_{in}/S))$, values as a function of calculated PAMPA membrane $\log P_m^{\text{PAMPA -BBB}}$

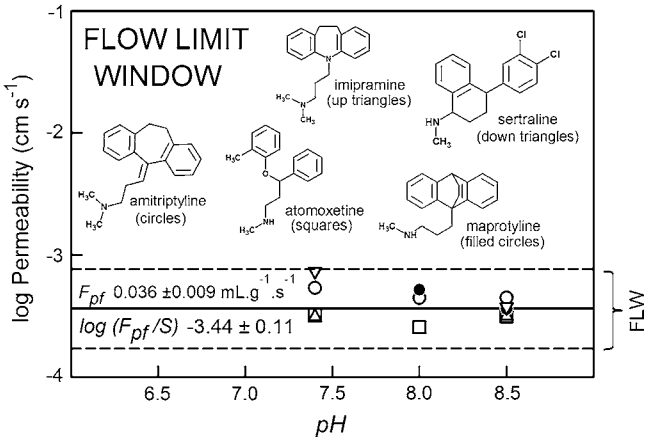

Fig. 3 The flow-limited permeability values of amitriptyline, atomoxetine, imipramine, maprotiline, and sertraline (12 points). The solid line represents the weighted mean log $(F_{pf}/S) - 3.44 \pm 0.11 (F_{pf} 0.036 \pm 0.009 \text{mL} \cdot \text{g}^{-1} \cdot \text{s}^{-1})$ based on 12 points. The dashed lines represent a range based on ±3 standard deviations, marking the proposed flow limit window (FLW) to be expected for data compiled from different laboratories.

(pH 7.4) permeability values (free of ABL effects). The *in situ* brain perfusion K_{in} data of mostly lipophilic drugs were taken from four sources—two based on rat: Summerfield *et al.* (11) and Obradovic *et al.* (13); two based on mouse: Dagenais *et al.* (12) and Zhao *et al.* (14). The infusion flow rate in the mouse assays, 2.5 mL·min $^{-1}$, produces practically the same cerebrovascular flow velocity (~0.04 mL·g $^{-1}$·s $^{-1}$) as does 20 mL·min $^{-1}$ in the rat

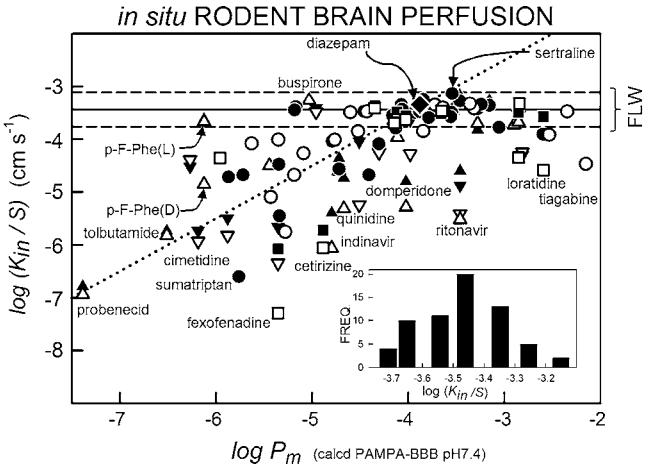

Fig. 4 The plot of 132 *in situ* brain perfusion log P_e (=log(K_{in}/S)) values as a function of calculated (*p*CEL-X) PAMPA membrane log $P_m^{\text{PAMPA-BBB}}$ (pH 7.4) permeability values (free of ABL effects). The data were taken from Summerfield *et al.* (11) (rat, circles, n=49), Obradovic *et al.* (13) (rat, squares, n=21), Dagenais *et al.* (12) (mouse, up-triangles, n=38), and Zhao *et al.* (14) (mouse, down-triangles, n=24). The average diazepam position is represented by the diamond symbol. The solid and dashed lines in Fig. 4 define the flow limit window (FLW) as in Fig. 3. The inset plot shows the frequency distribution of the 66 compounds bounded by the FLW. The dotted curve represents a unit slope line going through the diazepam point, suggesting the expected relationship between *in situ* and PAMPA data in the absence of hydrodynamic effects.

assays. The average diazepam log P_e= −3.35 (11,12) is represented by the diamond symbol. The highest log P_e (−3.14) reported is that of sertraline (11). The difference between log P_e of the two molecules, 0.21, is of the order of the expected inter-laboratory variance for *in situ* measurements and is about two times the standard deviation determined in the present analysis. The above sertraline value is greater than that reported by Dagenais *et al.* (12) by 0.32, a value again suggestive of the expected inter-laboratory variance.

The solid and dashed lines in Fig. 4 define the FLW as in Figure 3. Within this FLW, 66 of the 132 compounds (50%) may be considered flow-limited. If the Summerfield *et al.* (11) value of diazepam (−3.48) were selected as a flow marker, then 53% of the molecules in the FLW could not be corrected for flow (since $1 - K_{in}/F_{pf} < 0$). If the Dagenais *et al.* (12) value of diazepam (−3.38) were the designated flow marker, then 27% of the molecules could not be corrected for flow. These literature *in situ* rodent brain perfusion measurements highlight the quandary in the Crone-Renkin equation when it is applied to typical CNS drugs, which are often quite lipophilic.

The inset plot in Fig. 4 categorizes the frequency distribution of the 66 compounds bounded by the FLW. As can be seen, the highest number of flow-limited molecules has nearly the same value of K_{in} as that resulting from our own analysis. The distribution appears normal in shape.

The dotted curve in Fig. 4 represents a unit slope line going through the diazepam point, suggesting the expected relationship between *in situ* and PAMPA data in the absence of hydrodynamic effects. The high scatter of the points below the flow limit can be attributed in part to transporter effects: efflux (e.g., fexofenadine, cetirizine,

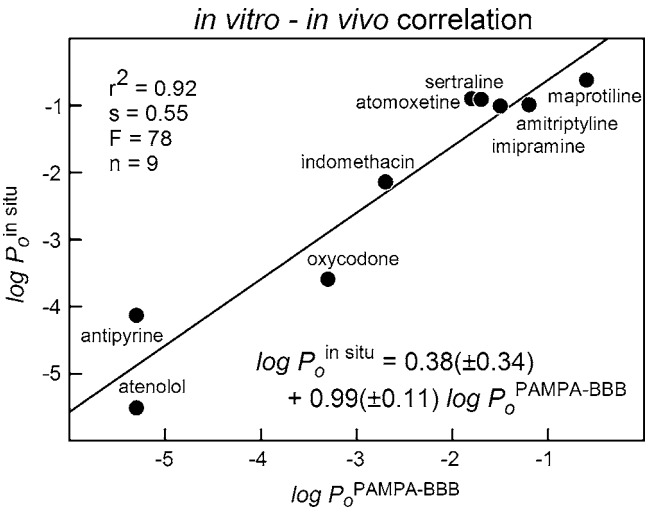

Fig. 5 The correlation plot of log $P_o^{in\ situ}$ as a function of log $P_o^{\text{PAMPA-BBB}}$, with the PAMPA measurements (Table I) based on porcine brain extract lipids (34).

indinavir, ritonavir, and quinidine) or carrier-mediated uptake (e.g., p-F-phenylalanine, L-enantiomer). The filled circles in Fig. 4 are associated with non-Pgp substrates, whereas the unfilled circles are compounds with efflux ratios >3 based on the MDCK-MDR1 cell model (11). The filled squares are K_{in} values determined in the presence of 5 μM CsA, whereas the unfilled squares are those measured without any inhibitor (13). The triangles correspond to mouse K_{in} values. Filled triangles are based on Pgp-knockout (KO; mdr1a(−/−)) mouse results; unfilled triangles are based on wild-type (WT) mice.

IVIVC Based on PAMPA and *In Situ* Intrinsic Permeability

Figure 5 shows the correlation plot of log $P_o^{in\ situ}$ as a function of log $P_o^{\mathrm{PAMPA-BBB}}$, with the PAMPA measurements (Table I) based on porcine brain extract lipids (34). The fitted slope is practically unit value, and the intercept is within one standard deviation of zero. With $r^2 = 0.92$, the PAMPA model appears robust, and may be used to predict log $P_o^{in\ situ}$ values of uncharacterized molecules for selecting the optimal pH values for the pH-CRE method, as recommended below.

pH-CRE Method Recommendations

Although any of the lipophilic bases studied here can be used as a flow marker at pH 7.4, maprotiline is recommended as a replacement for diazepam when lipophilic CNS drugs are studied. It is not only among the most permeable molecules characterized to date, but being a base with a secondary amine, it has a pK_a appreciably higher than those of the tertiary amines (Table I). This affords flexibility in the choice of pH for the K_{in} measurement to take advantage of the pH-CRE method. In addition to the pH 7.4 (normal KRB) measurement of K_{in}, a measurement in KRB + 10 mM MES, adjusted to pH 6.5, is recommended for maprotiline. If imipramine were selected, then the second buffer point could be pH 5.5 or 6.0, a little farther from the physiological pH, compared to maprotiline, but still within the plausible working pH range.

More generally, for any of the lipophilic bases considered here ($P_o >> F_{pf}/S$), it can be recommended that the pK_a^{flux} value be calculated from the 'flux-pK_a' equation (15) $\log P_o = \log(F_{pf}/S) + |pK_a - pK_a^{\mathrm{flux}}|$, where either the measured or predicted (e.g., *p*CEL-X) PAMPA-BBB intrinsic (P_o) permeability be used, along with $F_{pf}/S = 0.036/100$ cm·s^{-1}. That is, for a base, $pK_a^{\mathrm{flux}} \approx pK_a - \log P_o^{\mathrm{PAMPA-BBB}} - 3.44$. The optimal two buffer pH values may be selected to be (i) at the estimated pK_a^{flux} value and (ii) at about 1.7 pH units away (but within the pH 5.5–8.5 domain), in the direction of lower permeability, following the line of reasoning discussed in detail elsewhere (29). Two pH points are minimally sufficient, but more values would be advisable if the molecule is a suspected substrate for a carrier-mediated transport process (16).

CONCLUSION

It was shown by the analysis of the *in situ* rat brain perfusion measurements in the pH 6.5–8.5 interval for five lipophilic (log P_{OCT} 3.3–5.1) bases, confirmed by the analysis of 132 published rodent data as a function of passive permeability (PAMPA-BBB model), that for infusion flow rates used in several mouse and rat studies, the average cerebrovascular flow velocity $F_{pf} = 0.036 \pm 0.009 \mathrm{mL \cdot g^{-1} \cdot s^{-1}}$. The distribution of 66 literature permeability measurements of apparently flow-limited molecules can be used to define a "flow-limit window" (FLW), marked off by effective BBB permeability (not corrected for flow) $P_e^{\min} = 170$ and $P_e^{\max} = 776$ (10^{-6} cm·s^{-1} units), based on three times the standard deviation in the F_{pf} value determined here. The Crone-Renkin equation (CRE) using diazepam as a flow marker is expected not to work for half of the molecules in the FLW and is expected to underestimate the other half of the molecules, by up to a factor of 64 (sertraline, pH 8.5). It was shown that the pH-CRE flow correction method, based on the pH partition hypothesis, can overcome this limitation for ionizable drugs.

ACKNOWLEDGMENTS

We thank Drs. Feng Zhou and Ismael J. Hidalgo of Absorption Systems for their effort in the *in situ* brain perfusion measurements and for the valuable background discussions. The technical assistance of Oksana Tsinman (*p*ION) is gratefully acknowledged. Part of this work was supported by Grant Number R44MH75211 from the National Institutes of Health (to *p*ION). The content is solely the responsibility of the authors and does not necessarily represent the official views of the National Institute of Mental Health or the National Institutes of Health.

REFERENCES

1. Abbott NJ, Patabendige AA, Dolman DE, Yusof SR, Begley DJ. Structure and function of the blood-brain barrier. Neurobiol Discov. 2010;37:13–25.
2. Hammarlund-Udenaes M, Fridén M, Syvänen S, Gupta A. On the rate and extent of drug delivery to the brain. Pharm Res. 2008;25:1737–50.

3. Hitchcock SA. Blood-brain barrier permeability considerations for CNS-targeted compound library design. Curr Opin Chem Biol. 2008;12:1–6.
4. Jeffrey P, Summerfield SG. Challenges for blood-brain barrier (BBB) screening. Xenobiotica. 2007;37:1135–51.
5. Takasato Y, Rapoport SI, Smith QR. An *in situ* brain perfusion technique to study cerebrovascular transport in the rat. Am J Physiol. 1984;247:H484–93.
6. Smith QR. A review of blood-brain barrier transport techniques. Methods Mol Med. 2003;89:193–208.
7. Parepally JMR, Mandula H, Smith QR. Brain uptake of nonsteroidal anti-inflammatory drugs: ibuprofen, flurbiprofen, and indomethacin. Pharm Res. 2006;23:873–81.
8. Renkin EM. Capillary permeability to lipid-soluble molecule. Am J Physiol. 1952;168:538–45.
9. Crone C. The permeability of capillaries in various organs as determined by use of the "indicator diffusion" method. Acta Physiol Scand. 1963;58:292–305.
10. Crone C, Levitt DG. Capillary permeability to small solutes. In: Renkin EM, Michel CC, editors. Handbook of Physiology, Sec. 2: The Cardiovascular System. Bethesda: Amer. Physiol. Soc; 1984. p. 411–66.
11. Summerfield SG, Read K, Begley DJ, Obradovic T, Hidalgo IJ, Coggon S, *et al.* Central nervous system drug disposition: the relationship between *in situ* brain permeability and brain free fraction. J Pharmacol Exp Ther. 2007;322:205–13.
12. Dagenais C, Avdeef A, Tsinman O, Dudley A, Beliveau R. P-Glycoprotein deficient mouse *in situ* blood-brain barrier permeability and its prediction using an *in combo* PAMPA model. Eur J Pharm Sci. 2009;38:121–37.
13. Obradovic T, Dobson GG, Shingaki T, Kungu T, Hidalgo IJ. Assessment of the first and second generation antihistamines brain penetration and the role of P-glycoprotein. Pharm Res. 2007;24:318–27.
14. Zhao R, Kalvass JC, Pollack GM. Assessment of blood-brain barrier permeability using the *in situ* mouse brain perfusion technique. Pharm Res. 2009. doi:10.1007/S1105-009-9876-4. in press.
15. Avdeef A, Artursson P, Neuhoff S, Lazorova L, Gråsjö J, Tavelin S. Caco-2 permeability of weakly basic drugs predicted with the Double-Sink PAMPA pK_a^{flux} method. Eur J Pharm Sci. 2005;24:333–49.
16. Sugano K, Kansy M, Artursson P, Avdeef A, Bendels S, Di L, et al. Coexistence of passive and active carrier-mediated uptake processes in drug transport: a more balanced view. Nature Rev Drug Discov. 2010;9:597–614.
17. Evans CAN, Reynolds JM, Reynolds ME, Saunders NR. The effect of hypercapnia on a blood-brain barrier mechanism in foetal and new-born sheep. J Physiol. 1976;255:701–14.
18. Nagy Z, Szabo M, Huttner I. Blood-brain barrier impairment by low pH buffer perfusion via the internal carotid artery in rat. Acta Neuropathol. 1985;68:160–3.
19. Greenwood J, Hazell AS, Luthert PJ. The effect of a low pH saline perfusate upon the integrity of the enery-depleted rat blood-brain barrier. J Cereb Blood Flow Metab. 1989;9:234–42.
20. Okura T, Hattori A, Takano Y, Sato T, Hammarlund-Udanenaes M, Terasaki T, *et al.* Involvement of the pyrilamine transporter, a putative organic cation transporter, in blood-brain barrier transport of oxycodone. Drug Metab Dispos. 2008;36: 2005–13.
21. Avdeef A, Bucher JJ. Accurate measurements of the concentration of hydrogen ions with a glass electrode: calibrations using the Prideaux and other universal buffer solutions and a computer-controlled automatic titrator. Anal Chem. 1978;50:2137–42.
22. Avdeef A. Absorption and drug development. Hoboken: Wiley-Interscience; 2003.
23. Street JA, Hemsworth BA, Roach AG, Day MD. Tissue levels of several radio labelled beta-adrenoceptor antagonists after intravenous administration in rats. Arch Int Pharmacodyn Thér. 1979;237:180–90.
24. Wang Q, Rager JD, Weinstein K, Kardos P, Dobson GL, Li J, et al. Evaluation of teh MDR-MDCK cell line as a permeability screen for the blood-brain barrier. Int J Pharm. 2005;288:349–59.
25. Smith QR, Ziylan YZ, Robinson PJ, Rappoport SI. Kinetics and distribution volumes for tracers of different sizes in the brain plasma space. Brain Res. 1988;462:1–9.
26. Abbruscato TJ, Thomas SA, Hruby VJ, Davis TP. Blood-brain barrier permeability and bioavailability of a highly potent and μ-selective opioid receptor antagonist, CTAP: comparison with morphine. J Pharmacol Exp Ther. 1997;280:402–9.
27. Ohno K, Pettigrew KD, Rapoport SI. Lower limits of cerebrovascular permeability to nonelectrolytes in the conscious rat. Am J Physiol. 1978;235:H299–307.
28. Avdeef A. Leakiness and size exclusion of paracellular channels in cultured epithelial cell monolayers—interlaboratory comparison. Pharm Res. 2010;27:480–9.
29. Ruell JA, Tsinman KL, Avdeef A. a drug absorption *in vitro* model. 5. Unstirred water layer in iso-pH mapping assays and pK_a^{flux}—optimized design (*p*OD-PAMPA). Eur J Pharm Sci. 2003;20:393–402.
30. Avdeef A, Nielsen PE, Tsinman O. a drug absorption *in vitro* model. 11. Matching the *in vivo* unstirred water layer thickness by individual-well stirring in microtitre plates. Eur J Pharm Sci. 2004;22:365–74.
31. Avdeef A, Kansy M, Bendels S, Tsinman K. Absorption-excipient-pH classification gradient maps: sparingly-soluble drugs and the pH partition hypothesis. Eur J Pharm Sci. 2008;33:29–41.
32. Avdeef A, Tsinman O. Miniaturized rotating disk intrinsic dissolution rate measurement: effects of buffer capacity in comparisons to traditional Wood's apparatus. Pharm Res. 2008;25:2613–27.
33. Fagerberg JH, Tsinman O, Tsinman K, Sun N, Avdeef A, Bergström CAS. Dissolution Rate and Apparent Solubility of Poorly Soluble Compounds in Biorelevant Dissolution Media. Mol Pharm. 2010, June 24 *Epub ahead of print.*
34. Tsinman O, Tsinman K, Sun N, Avdeef A. Physicochemical selectivity of the BBB microenvironment governing passive diffusion—matching with a porcine brain lipid extract artificial membrane permeability model. Pharm Res. 2010, in press.
35. Murakami H, Takanaga H, Matsuo H, Ohtani H, Sawada Y. Comparison of blood-brain barrier permeability in mice and rats using *in situ* brain perfusion technique. Am J Physiol Heart Circ Physiol. 2000;279:H1022–9.
36. Chikhale EG, Burton PS, Borchardt RT. The effect of verapamil on the transport of peptides across the blood-brain barrier in rats: kinetic evidence for an apically polarized efflux mechanism. J Pharmacol Exp Ther. 1995;273:298–303.
37. Pardridge WM, Triguero D, Yang J, Cancilla PA. Comparison of *in vitro* and *in vivo* models of drug transcytosis through the blood-brain barrier. J Pharmacol Exp Ther. 1990;253:884–91.
38. Liu X, Tu M, Kelley RS, Chen C, Smith BJ. Development of a computational approach to predict blood-brain barrier permeability. Drug Metab Dispos. 2004;32:132–9.
39. Cisternino S, Rousselle C, Debray M, Scherrmann J-M. *In situ* transport of vinblastine and selected P-glycoprotein substances: implications for drug-drug interactions at the mouse blood-brain barrier. Pharm Res. 2004;21:1382–9.